Journal of Volcanology and Geothermal Research 194 (2010) 174–188

Contents lists available at ScienceDirect

Journal of Volcanology and Geothermal Research

journal homepage: www.elsevier.com/locate/jvolgeores

The Luingo caldera: The south-easternmost collapse caldera in the Altiplano–Puna plateau, NW Argentina

Silvina Guzmán [a,*], Ivan Petrinovic [b]

[a] CONICET-IBIGEO, Museo de Ciencias Naturales, Universidad Nacional de Salta. Mendoza 2, (4400) Salta, Argentina
[b] CICTERRA-FCEFyN, Universidad Nacional de Córdoba, Av. Vélez Sarsfield 1611, X5016GCA, Córdoba, Argentina

ARTICLE INFO

Article history:
Received 27 November 2009
Accepted 19 May 2010
Available online 2 June 2010

Keywords:
collapse caldera
Cerro Galán
Southern Central Volcanic Zone
Miocene volcanism
Luingo caldera

ABSTRACT

This article identifies the Pucarilla–Cerro Tipillas Volcanic Complex and its major eruptive source, the Luingo caldera (26° 10′S–66° 40′W). Detailed geological mapping, stratigraphic sections, facies analysis and correlations, including the identification of typical caldera components, allow us to infer the position of a collapse caldera, elongated at N65° and with a diameter of 19 km × 13 km, which is responsible for an eruption of 135 km^3 (DRE) of magma. The high-crystal contents of the associated ignimbrites, combined with its tectonic setting, indicate that regional and local tectonic structures played a crucial role in the formation of the caldera.

The Luingo caldera is located on the south-eastern border of the Puna, and is the south-easternmost recognised caldera of the Altiplano–Puna plateau. The age of the caldera and its products is 12.1 to 13.5 Ma. Based on its location near the Cerro Galán Complex (2 to 6.5 Ma), we can imply that volcanism existed in the area for about 10 Ma. The caldera morphology and product distribution account for a middle Miocene paleao-topography similar to the present one.

1. Introduction

The number of studies of large collapse calderas in the Central Andes and their silicic products has increased notably in the last decade (e.g., de Silva, 1989; Ort, 1993; Petrinovic et al., 1999; Lindsay et al., 2001a, b; Soler et al., 2007; Petrinovic et al., 2010).

At present, 20 major collapse calderas have been recognised in the 28°–18° S segment (Fig. 1) of the Central Volcanic Zone (CVZ: 28–14° S Thorpe et al., 1984; de Silva and Francis, 1991). They are concentrated between 21° and 25° S and include the well known Altiplano–Puna Volcanic Complex (APVC: de Silva, 1989), where large ignimbritic fields and calderas have been the focus of several studies (e.g., de Silva, 1989; Ort, 1993; Lindsay et al., 2001a, b; Soler et al., 2007). In contrast, few detailed studies have been conducted of the ignimbrites within the Southern CVZ (25–27°S), where there are few recognised vents. Between 67 and 69°W, these ignimbrites are characterised as small to medium in volume (<10 km^3) and have crystal-poor felsic compositions (e.g., Siebel et al., 2001; Schnurr et al., 2007). One exception is the large-volume Cerro Galán caldera to the east, which ignimbrites are dacitic and crystal-rich, similar to many of the ignimbrites of the APVC.

To gain knowledge of the Southern CVZ volcanic sources and products, we have studied the Pucarilla–Cerro Tipillas Volcanic Complex (PCTVC) in the south-eastern Puna border. This complex is composed of vast pyroclastic deposits and minor lava flows that until now remained unrelated to any known vent. This study identifies an older caldera-forming episode, the Luingo caldera, within the Cerro Galán caldera area (Francis et al., 1980; Sparks et al., 1985). We include field characteristics and facies analysis of deposits of the Luingo caldera, as well as new isotopic ages and volume computations.

The Luingo caldera's volcanic structure and its products become the south-easternmost of the Altiplano–Puna plateau. The spatial and temporal relationship of the Luingo caldera to the Cerro Galán caldera suggests a recurrent and protracted volcanism, including similar characteristics in a reduced area which was strongly conditioned by magma input, storage, and favourable eruption conditions. Additionally, ash-fall deposits interbedded in sedimentary sequences near the volcanic source, which are approximately the same age as the Luingo caldera, allow us to evaluate the two for a possible relationship.

2. Geological background and tectonic setting

The stratigraphy of the volcanic units of the PCTVC has been proposed by González et al. (1999) and Hongn and Seggiaro (2001). Reported ages in the area include 12.11 ± 0.11 Ma (Marrett et al., 1994) for the Pucarilla Ignimbrite and 15.83 ± 0.44 Ma to 14.22 ± 0.33 Ma for the Hornblendic welded tuff (Sparks et al., 1985). These ignimbrites have been correlated by González et al. (1999) and Hongn and Seggiaro (2001). This article unifies the stratigraphy above. The

* Corresponding author. Museo de Ciencias Naturales, Mendoza No. 2 (4400)-Salta, Argentina. Tel./fax: +54 387 431 8086.
E-mail address: sguzman@unsa.edu.ar (S. Guzmán).

0377-0273/$ – see front matter © 2010 Elsevier B.V. All rights reserved.
doi:10.1016/j.jvolgeores.2010.05.009

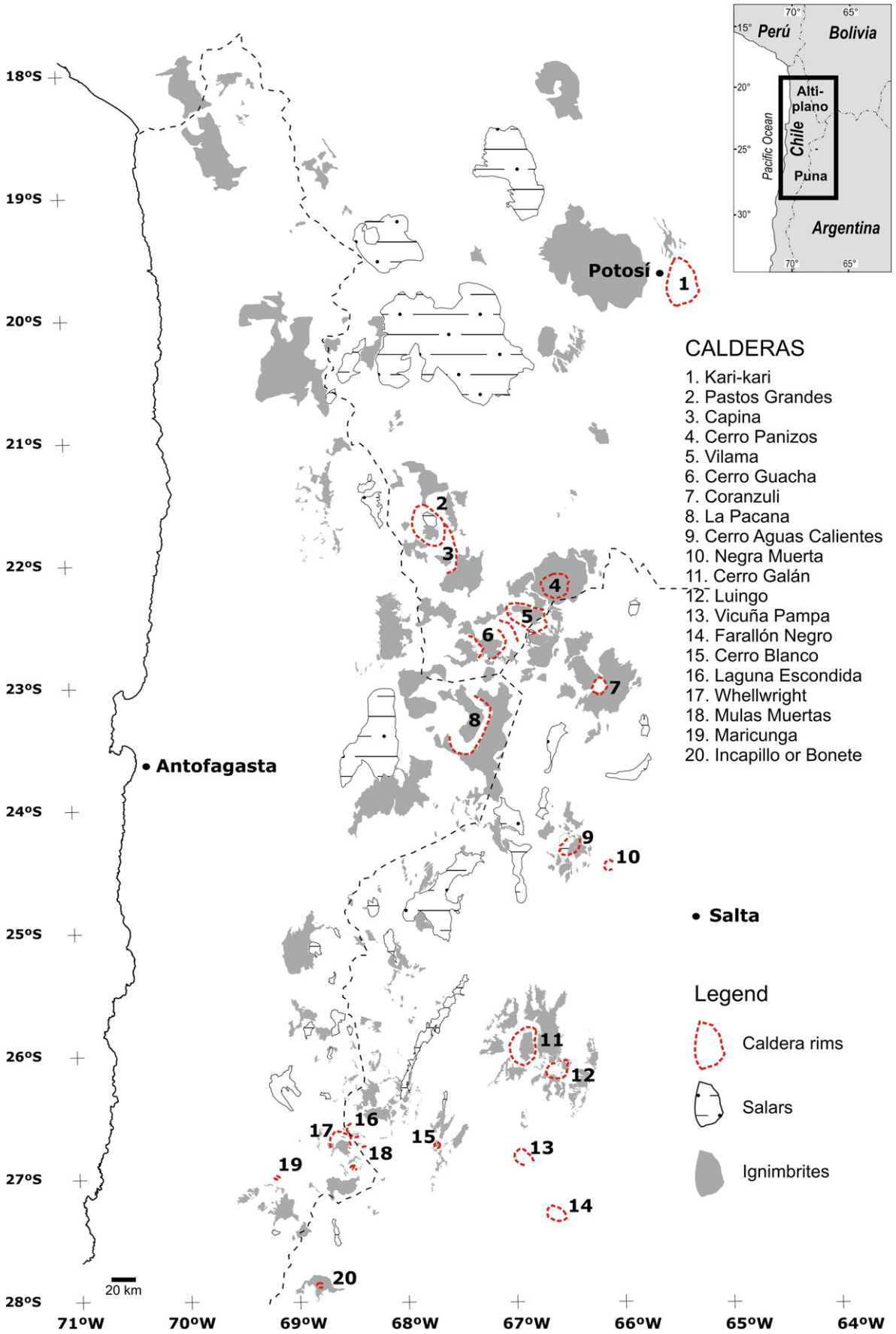

Fig. 1. Regional map of the 18–28°S segment of the Central Andes Central Volcanic Zone (modified from Petrinovic et al., 2010), showing the present understanding of the distribution of ignimbrites and calderas.

Table 1
Former naming of the units related to PCTVC and the ones suggested in this work.

	Former naming	Distribution	Brief description	Former assigned age	Reference	Suggested naming
Generic denomination including large areas	Laguna Blanca Formation	W of El Cajón Range	Dacitic tuffs	Lower Quaternary	Turner (1962)	Units of the PCTVC (when present in the area assigned to PCTVC)
	Laguna Blanca Formation: Tobas dacíticas	Between El Cajón and Carachipampa ranges	Dacitic tuffs	Lower Quaternary? Upper Tertiary?	Navarro García (1984)	
	Andesitas y dacitas Tebenquicho	Broadly Spread in the southern portion of Puna	Andesitic and dacitic lavas	Middle Miocene (10–15 Ma)	González (1992)	
Specific denominations	Flujos Ignimbríticos	South of Hualfín Valley	Dacitic welded tuffs	Quaternary	Castillo and Aguilera (1988)	Pucarilla Ignimbrite
	Welded Tuff	Around Jasimaná fault	Welded tuff	12.11 ± 0.11 Ma	Marrett et al. (1994)	
	Pucarilla Ignimbrite	Near Hualfín	Dacitic tuff	Middle Miocene	Hongn and Seggiaro (2001)	
	Pampallana Ignimbrite	South of Pampallana	Andesitic tuff	Middle Miocene	González et al. (1999)	
	Hornblendic welded tuff/old hornblende welded tuff	Eastern flanks of Cerro Galán Caldera	Welded tuff	14.22 ± 0.33 to 15.83 ± 0.44 Ma	Sparks et al. (1985)	Alto de Las Lagunas Ignimbrite

Pucarilla–Cerro Tipillas Volcanic Complex consists of deposits that were previously assigned to the Laguna Blanca Formation (Turner, 1962), *Tobas dacíticas* (Navarro García, 1984), hornblendic welded tuff (Sparks et al., 1985), *flujos ignimbríticos* (Castillo and Aguilera, 1988), *andesitas y dacitas Tebenquicho* (González, 1992), Ignimbrita Pucarilla (Hongn and Seggiaro 2001), Ignimbrita Pampallana (González et al., 1999), and *Basalto Antiguo* and *Andesitas Viejas* (González, 1992). The stratigraphic correlations and the new names proposed are shown in Table 1.

Units from the PCTVC unconformably overlie sediments of the Payogastilla Group (Díaz and Malizzia, 1984) and more precisely, of the fluvial Angastaco Formation (Camacho de Alcalde, 1977). In the studied area, only the basal-middle sections of this formation have been identified; its middle Miocene age (Grier and Dallmeyer, 1990; Pereyra et al., 2008) is constrained by the presence of three interbedded tuffs. The interbedded tuffs are approximately coeval with the ages determined by Sparks et al. (1985) and Marrett et al. (1994) for the PCTVC.

In other sections, the PCTVC covers the local Neoproterozoic–Palaeozoic basement, and includes medium- to high-grade metamorphic rocks, such as the La Paya Formation (Aceñolaza et al., 1976), the Río Blanco Metamorphic Complex (e.g., Hongn and Seggiaro, 2001) and the Loma Corral Formation (Navarro García, 1984), granitoids of the Oire Eruptive Complex (Blasco and Zappettini, 1996), and the Peñas Blancas Granite (Castillo, 1999). The Peñas Blancas Granite could also be included within the Oire Eruptive Complex, as it is similar to leucogranites found in this complex described by Viramonte et al. (2007).

The PCTVC is located on the Puna border, on the boundary with the Eastern Cordillera, and marks the eastern limit of the large-volume Cenozoic magmatism found in the Altiplano–Puna plateau. Most of the PCTVC deposits are located in the southern prolongation of the Colomé–Hualfín Valley (Fig. 2). This valley, consistent with most in the Puna region, is bounded by regional faults with opposite vergence. The western fault thrusts basement rocks onto the Payogastilla Group, whereas the eastern fault (Jasimaná Fault: Marrett et al., 1994) reflects a Neogene inversion of a previous normal fault (e.g., Seggiaro et al., 2006; Carrera and Muñoz, 2008) and marks the western limit of the Cretaceous Salta rift (e.g., Hongn and Seggiaro, 2001; Mortimer et al., 2007) and the eastern limit of the PCTVC. Seggiaro et al. (2006) show that this reverse NW–SE trending fault has an oblique left-lateral component. The deposits of the PCTVC are now affected by a reactivation of the Jasimaná fault (e.g., Marrett et al., 1994; Seggiaro et al., 2006; Guzmán, 2009); nevertheless, at the time of the major PCTVC eruption (13.5–12 Ma) this area served as a topographic barrier, as no deposits or clasts of this complex have been preserved in the middle Miocene sedimentary sequence to the east of this master fault. The presence of a topographic high in this area in middle Miocene time has been previously suggested by Coutand et al. (2006), based on other evidence.

Other faults to the west (Fig. 2) have similar trends as the Jasimaná fault (Fig. 2), including left-lateral oblique components and the same western vergence (Guzmán, 2009). It is noteworthy that some of these faults were active before the PCTVC major eruptive event and other faults after it (Guzmán, 2009).

The boundary between the Puna, the Eastern Cordillera and the Sierras Pampeanas is a highly deformed belt which has been active since the Proterozoic (Hongn et al., 2008). Different basement lithologies in contact through the master fault planes are covered by syn-deformational sedimentary rocks from the Cretaceous rift basin (e.g., Seggiaro et al., 2006) and the Eocene–Miocene foreland basin (Hongn et al., 2008). Taking these conditions into consideration, the successive reactivation of basement anisotropies (Hongn et al., 2008) has played a significant role in the structural configuration of the area.

3. PCTVC stratigraphy

Here we define new stratigraphic units and redefine previously named units. The PCTVC includes pyroclastic and effusive deposits which are divided into units. The discrimination between the different volcanic units is mainly based on field characteristics, stratigraphic relationships, petrographic aspects, and chemical composition. The Pucarilla Ignimbrite is then subdivided based on lithofacies variations. Stratigraphic sections of particular sites are shown in Fig. 3; three generalised sections of the recognised volcanic units are represented in Fig. 4.

3.1. Alto de Las Lagunas Ignimbrite

Based on the well-exposed outcrops in the surroundings of Alto de Las Lagunas, we rename the hornblendic welded tuff of Sparks et al. (1985) as the Alto de Las Lagunas Ignimbrite. The base of this ignimbrite has not been observed; its maximum observed thickness is 80 m and it is commonly covered either by Lavas II (see below) or by the Cerro Galán Ignimbrite (Sparks et al., 1985). We have determined a new age of 13.52 ± 0.12 Ma (Table 2; Appendix A), which is younger than previously reported ages (c.f., Sparks et al., 1985). There is no evident stratigraphic relationship between the Alto de Las Lagunas Ignimbrite and the other units of the PCTVC, but this new date indicates that this ignimbrite initiated the PCTVC sequence. It is a pink

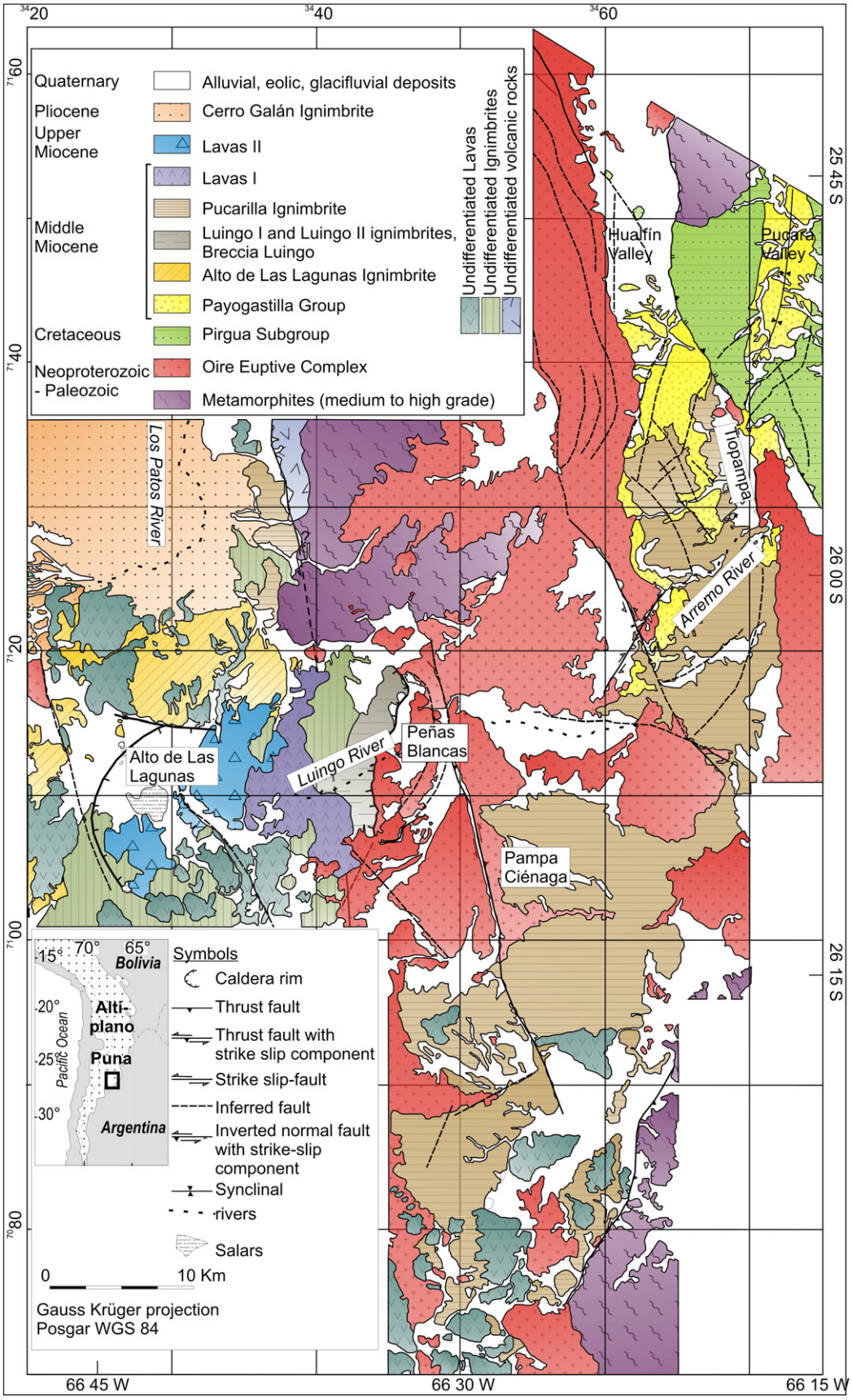

Fig. 2. Geologic map of the Pucarilla–Cerro Tipillas Volcanic Complex and the surrounding area.

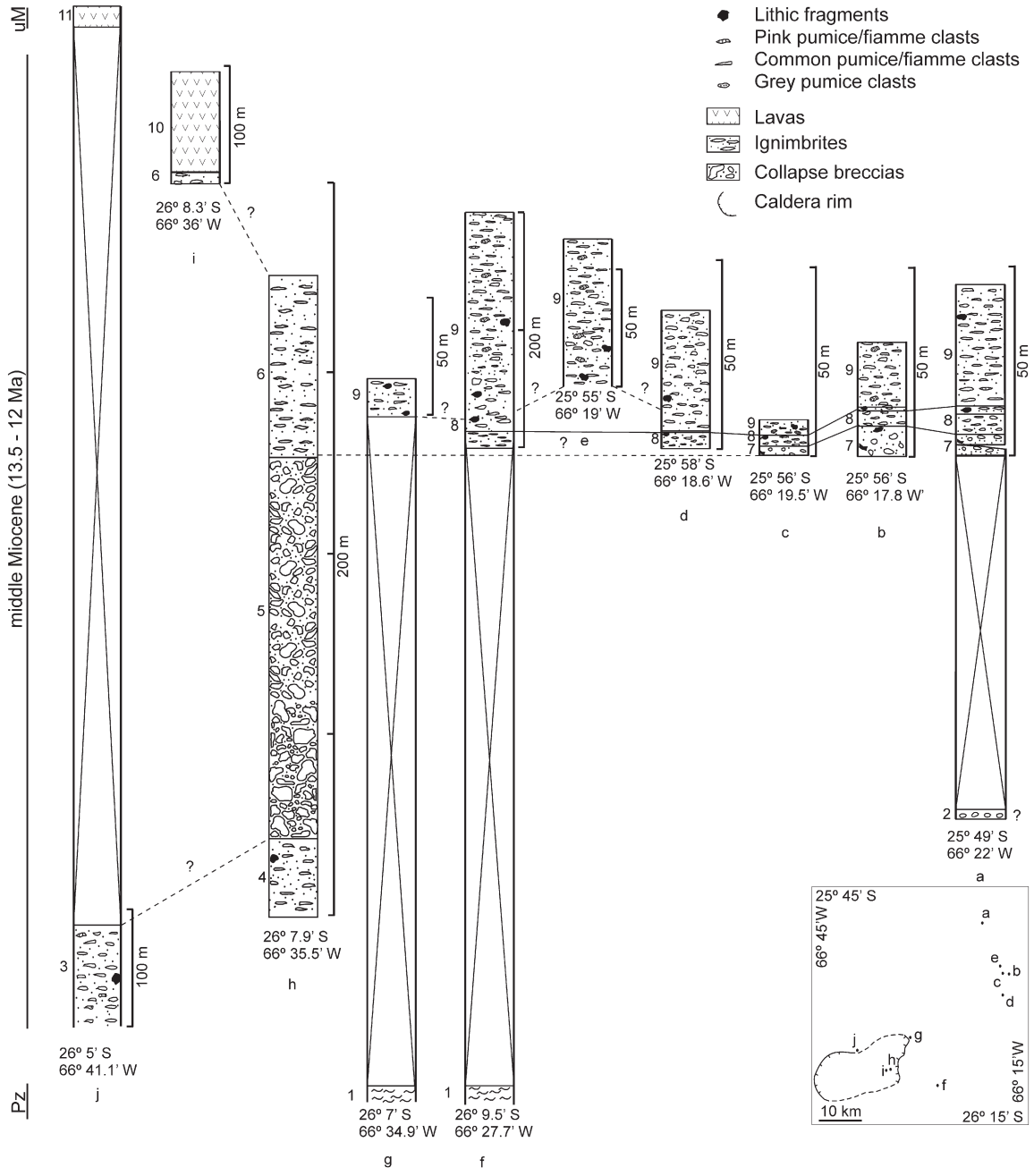

Fig. 3. Measured stratigraphic sections of the PCTVC showing correlation lines. uP: upper Miocene; Pz: Paleozoic. 1) Paleozoic basement, 2) Angastaco Formation, 3) Alto de Las Lagunas Ignimbrite, 4) Luingo I Ignimbrite, 5) Luingo Breccia, 6) Luingo II Ignimbrite, 7) Hualfín Unit, 8) Arremo Unit, 9) Jasimaná Unit, 10) Lavas I, 11) Lavas II.

to grey colour, intensely welded and devitrified, massive lapilli tuff. Three varieties of vesiculated clasts are recognised; the most abundant type is a grey, crystal-rich (~30 vol.%) fiamme that forms about 20 vol.% of the deposit volume, a variety of pink pumice clasts (altered and flattened, with about 50 vol.% of crystals) are scarce (<2 vol.%), as are grey crystal mush clasts (vesicle poor, with up to 90% of crystals). Lithic fragments of Palaeozoic granitoids are below 1 vol.%. The ignimbrite is dacitic and crystal-rich (35 vol.%) with plagioclase, alkaline feldspar, quartz, amphibole and biotite, and with accessory phases of sphene, apatite, zircon and Ti–Fe oxides.

3.2. Pucarilla ignimbrite

Originally defined by Hongn and Seggiaro (2001), the Pucarilla Ignimbrite is a medium- to high-grade dacitic ignimbrite with an intense to (less commonly) moderate degree of welding. The ignimbrite is crystal-rich (15 to 38 vol.% in pumice and 32 to 48 vol.% in matrix, see Fig. 5) and has a low lithic content (<3 vol.%). Pumice contents vary between 10 and 40 vol.%, but generally are between 20 and 30 vol.%. Vesiculated fragments can be divided into three types: 1) most prominent are common pumice clasts, which vary in colour from white to black based on the degree of welding, 2) pink pumice clasts which are flattened (fiamme) and crystal-rich and 3) grey crystal mush clasts which are crystal-rich (up to 90 vol.% crystal content) and vesicle poor. It is important to note that the grey crystal mush fragments are interpreted as cognate fragments, representing side-wall accumulations of early crystallised (c.f. Lindsay et al., 2001b) but still are not solidified fractions. The mineral assemblage of this ignimbrite is plagioclase, clinopyroxene, biotite, quartz with accessory minerals sphene, magnetite, zircon and apatite. Based on observed

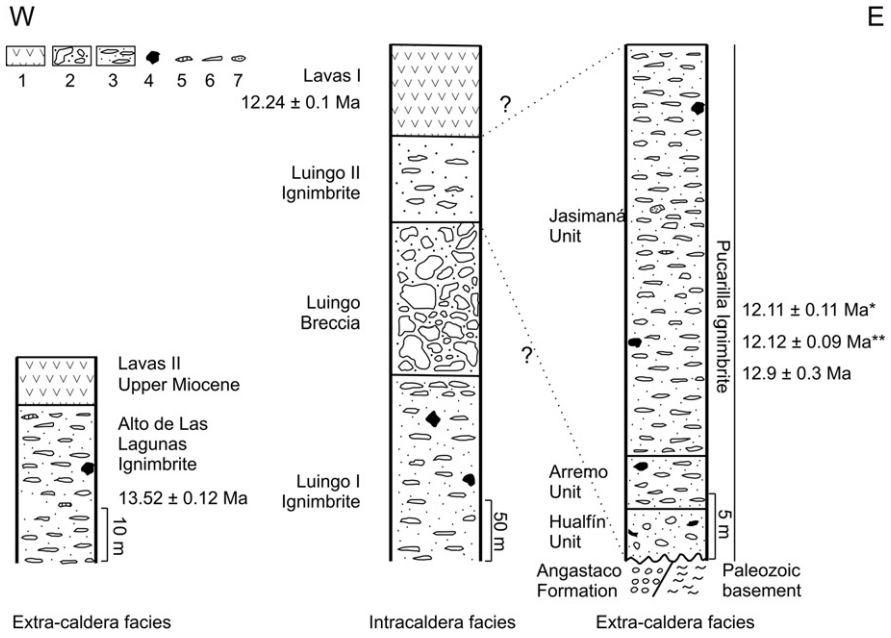

Fig. 4. Generalised sections of volcanic sequences from the PCTVC. 1) Lavas, 2) breccias, 3) ignimbrites, 4) lithic fragments, 5) pink fiamme, 6) common fiamme/pumices, 7) grey crystal mush clasts. Ages are from this contribution, except *Marrett et al. (1994), **Folkes et al. (submitted for publication).

lithofacies variations, the Pucarilla Ignimbrite is subdivided from base to top into the Hualfín, Arremo and Jasimaná units, described below.

3.2.1. Hualfín Unit

The Hualfín Unit is the lowermost of the Pucarilla Ignimbrite and is exposed only in a few sections. Identified outcrops are located at Hualfín, around Tiopampa, and on the western margin of the Los Patos River (Fig. 2). Its thickness varies from <1 m to a maximum of 6 m and it is whitish-grey in colour. The Hualfin Unit is a medium-grade ignimbrite which shows a variable welding degree, ranging from moderate to low, and constitutes a massive lapilli tuff (Fig. 6a) with a medium to fine ash matrix. Common pumice clasts are white; their content is highly variable throughout the section, from 10 to 20 vol.%. They are sub-rounded and their major axes length varies from less than 0.1 to 16 cm, showing some degree of flattening (Fig. 6b) with maximum strain ratios of 6:1. Grey crystal mush clasts and pink pumice clasts are fine grained and scarce (<1 vol.%). The grey crystal mush clasts are commonly incorporated inside the white pumice clasts. Lithic fragments of granitoids are scarce (<1 vol.%), sub-rounded to sub-angled, and do not exceed 2.2 cm. The crystal content of the pumices varies between 15 and 35 vol.% and between 33 and 45 vol.% in the matrix (Fig. 5).

3.2.2. Arremo Unit

The Arremo Unit overlies the Hualfín Unit. We obtained an age of 12.9 ± 0.3 Ma for this unit (see Table 2; Appendix A). It is well-exposed at the Arremo River (Fig. 2); exposure also occurs at Hualfín, Tiopampa, Pampa Ciénaga and on the margins of the Los Patos River. This medium-

Table 2
Ages > 7.4 Ma in the Cerro Galán area, from the literature and from this work.

Unit	Sample description	Method	Mineral	Sample	Location	Age ± 2σ errors (Ma)
	Ignimbrites	K–Ar	Whole rock		Peñas Blancas area	7.4 ± 0.3[a]
	Lavas (dacites)	K–Ar		G26	Cerro Galán area	9.9[b]
	Lavas (dacites)	K–Ar		G30	Cerro Galán area	10.4[b]
Lavas I	Lavas (dacites)	$^{40}Ar/^{39}Ar$	Biotite	CMS-21	26 08 35.6 S, 66 36 24.1 W	12.24 ± 0.1[c]
Pucarilla Ignimbrite (Jasimaná Unit)	Welded tuff (whole rock)	$^{40}Ar/^{39}Ar$	Biotite, Plagioclase		~25 52.5 S, ~66 19.5′W	12.11 ± 0.11[d]
Pucarilla Ignimbrite (Jasimaná Unit)	Dacite (pumice)	$^{40}Ar/^{39}Ar$	Biotite	P-002	25 54 31.1 S, 66 19 29.4 W	12.12 ± 0.09[e]
Pucarilla Ignimbrite (Arremo Unit)	Dacite (whole rock)	$^{40}Ar/^{39}Ar$	Biotite	N-02	25 56 9.4 S, 66 17 50.9 W	12.9 ± 0.3[c]
Alto de Las Lagunas Ignimbrite	Dacite (whole rock)	$^{40}Ar/^{39}Ar$	Biotite	CMS-38	26 05 13.7 S, 66 41 15.7 W	13.52 ± 0.12[c]
	Ignimbrites	K–Ar	Whole rock		Peñas Bancas area	13 ± 1[a]
Alto de Las Lagunas Ignimbrite	Hornblendic welded tuff (whole rock)	Rb–Sr	Biotite	SS168	Eastern flanks of Cerro Galán Caldera	14.22 ± 0.33[f]
Alto de Las Lagunas Ignimbrite	Old hornblende welded tuff (whole rock)	K–Ar	Biotite	SS 168	Eastern flanks of Cerro Galán Caldera	14.75 ± 0.40[f]
Alto de Las Lagunas Ignimbrite	Old hornblende welded tuff (whole rock)	K–Ar	Biotite	SS 168	Eastern flanks of Cerro Galán Caldera	15.83 ± 0.44[f]

[a] Castillo (1999).
[b] Francis et al. (1980) ages by Kretzschmar.
[c] This work.
[d] Marrett et al. (1994) average of 6 dates, location and identification of Unit pers. comm.
[e] Folkes et al. (submitted for publication).
[f] Sparks et al. (1985).

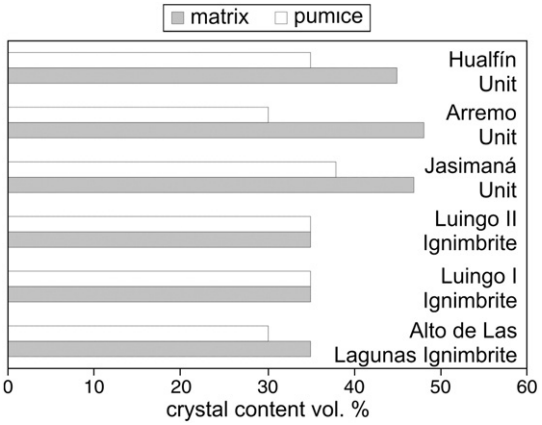

Fig. 5. Diagram showing crystal content (vol.%) found within pumices and in the matrix of ignimbrites.

to high-grade ignimbrite has a maximum thickness of 4 m. It is a grey massive lapilli tuff with a matrix of medium to fine sized ash. It has a medium-to-high degree of welding and intense devitrification showing a conspicuous eutaxitic texture (Fig. 6c) with imbricated fiamme. Most pumiceous fragments are black and are obsidian-like (c.f., Ross and Smith, 1961) fiamme, making up 20 to 40 vol.% of the deposit. The major fiamme axes vary from 0.5 to 20 cm, with strain ratios of up to 15:1. Pink fiamme and sub-rounded grey crystal mush clasts are scarce (<1 vol.%), the latter also occur in the common black fiamme (Fig. 6d). Lithic fragments are rare (<1 vol.%) and consist of grey and pink sub-rounded to sub-angular granitoids. Pumice crystal content reaches 30 vol.% and is between 32 and 48 vol.% in the matrix (Fig. 5).

3.2.3. Jasimaná Unit

This is the most widely distributed unit of the Pucarilla Ignimbrite and constitutes the top of the sequence with up to 205 m in thickness. This moderate to high-grade ignimbrite spreads through much of the area of the PCTVC. Ages of 12.11 ± 0.11 Ma (Marrett et al., 1994) and 12.12 ± 0.09 Ma (Folkes et al., unpublished) have been reported for this unit (Table 2). The eastern portion of the complex, from Hualfín to Pampa Ciénaga, has been surveyed, but it probably spreads farther south, as shown in Fig. 2, based on the interpretation of satellite images and descriptions contained in previous works (e.g., Navarro García, 1984; Castillo and Aguilera, 1988; González et al., 1999). Small outcrops have also been identified to the northeast and to the west of Alto de Las Lagunas (Fig. 2). The Jasimaná Unit is a pink, massive, highly welded (Fig. 6e) and devitrified lapilli tuff, where at least five cooling units are identified; columnar jointing is common. The high degree of welding persists both vertically and laterally. In a few places the ignimbrite is spherulitic (c.f., Mc Arthur et al., 1998), but devitrification textures, such as spherulites, are more abundant inside the pumice fragments, where primary porosity is greater. The most common fiamme are generally grey and their abundance ranges from 15 to 35% of the total deposit volume; their major axes reach 17 cm. Their strain ratios are generally less than 10:1, but sometimes reach 20:1. Grey and pink pumice clasts (Fig. 6f) are subordinate (<1 vol.%). The ignimbrite is crystal-rich, with 20 to 38 vol.% in pumice fragments and 35 to 47 vol.% in the matrix (see Fig. 5). Lithic fragments are rare (<1 vol.%), and where present are grey and pink sub-rounded to sub-angular granitoids.

3.3. Luingo I Ignimbrite

The Luingo I Ignimbrite is confined to the west of Peñas Blancas (Fig. 2). Its base is not exposed; the minimum thickness is approximately 120 m. It is a crystal-rich (~35 vol.%) intensely welded ignimbrite, green to grey coloured due to hydrothermal alteration (Fig. 7a), and displays well-developed columnar jointing in almost all its extent (Fig. 7b). The volume of the flattened pumiceous fragments is between 5 and 18%, with volume increasing towards the top of the sequence. The fragments are green to white, and are correlated, with variations in both alteration and porosity degrees. Maximum size ranges from 9 cm to, exceptionally, 19 cm. Lithic fragments are <3% in volume. Compositionally it is dacitic; the mineral association is plagioclase, clinopyroxene, chloritised biotite, and apatite, zircon, Fe–Ti oxides and sphene as accessory phases.

3.4. Luingo Breccia

Overlying the Luingo I Ignimbrite is the Luingo Breccia. Luingo Breccia has a total thickness of 100 m and is laterally distributed in a restricted area of 300 m. The deposit is a grey, massive and consolidated breccia (Fig. 7c and d). It is composed of fragments of granitoids from the host rock which are sub-rounded to angular, varying from 1 cm to more than 1 m in diameter. The matrix is a microbreccia, which has the same composition as the clasts and increases in abundance from 5 vol.% at the base to 30 vol.% at the top.

3.5. Luingo II Ignimbrite

This ignimbrite overlies the Luingo Breccia in the surroundings of the Luingo River and the Palaeozoic basement at Peñas Blancas (Fig. 2). It has a maximum thickness of 70 m. This crystal-rich (35 vol.%, see Fig. 5) ignimbrite is pale grey and slightly stratified at the base; towards the top it becomes darker and more indurated due to higher degrees of welding. Fiamme content varies from 4 to 7 vol.% and reaches from 5 to 10 cm in size, with a mean size of 1 cm. The strain ratio increases towards the top of the sequence to 10:1. Lithic fragments of sub-angular to sub-rounded granitoids (and less commonly volcanic fragments) constitute less than 1 vol.%. It has a dacitic composition, with a mineral association of plagioclase, chloritised biotite, quartz and minor clinopyroxene, and as accessories sphene, Ti–Fe oxides, zircon and apatite. Crystals found in the Luingo II Ignimbrite are larger than in other units (4 mm).

3.6. Hydrothermal breccias

In the SW border of the Alto de Las Lagunas depression (Fig. 2) a red to yellowish breccia delineates an arcuate 10-m thick hydrothermal dyke. The dyke propagates laterally and discontinuously for at least 100 m; its thickness typically changes laterally. The breccia is composed of sub-rounded to sub-angular individual crystal grains and lithic fragments of volcanic composition, all of them intensely silicified.

3.7. Lava flows

Restricted lava flows are distributed within the Alto de Las Lagunas depression, its surroundings, and in the margins of the Luingo River (Fig. 2). Vents were not recognised; the flows are probably related to flat and eroded lava domes or to effusive fissures. These lavas can be differentiated based on their stratigraphic relations, areal distribution, chemical composition, and absolute ages. Lavas I are andesitic and are distributed near the Luingo River. They overlie the Luingo II Ignimbrite and yield an age of 12.24 ± 0.1 Ma (see Table 2; Appendix A). Lavas II are dacitic and are distributed around and within the Alto de Las Lagunas depression. Preliminary data suggests an upper Miocene age (Guzmán et al., unpublished). Thus, we consider Lavas II as a separate eruptive episode, which is spatially associated with the 13.5–12.1 Ma episode.

3.8. Tuffs interbedded in middle Miocene sedimentary sequences

Interbedded in the Payogastilla Group continental sequence are continuous ash-fall deposits >2 m thick, with reported ages between 15.26 ± 0.23 Ma (Pereyra et al., 2008) and 13.4 ± 0.4 Ma (Grier and Dallmeyer, 1990). These tuffs were compared with the PCTVC

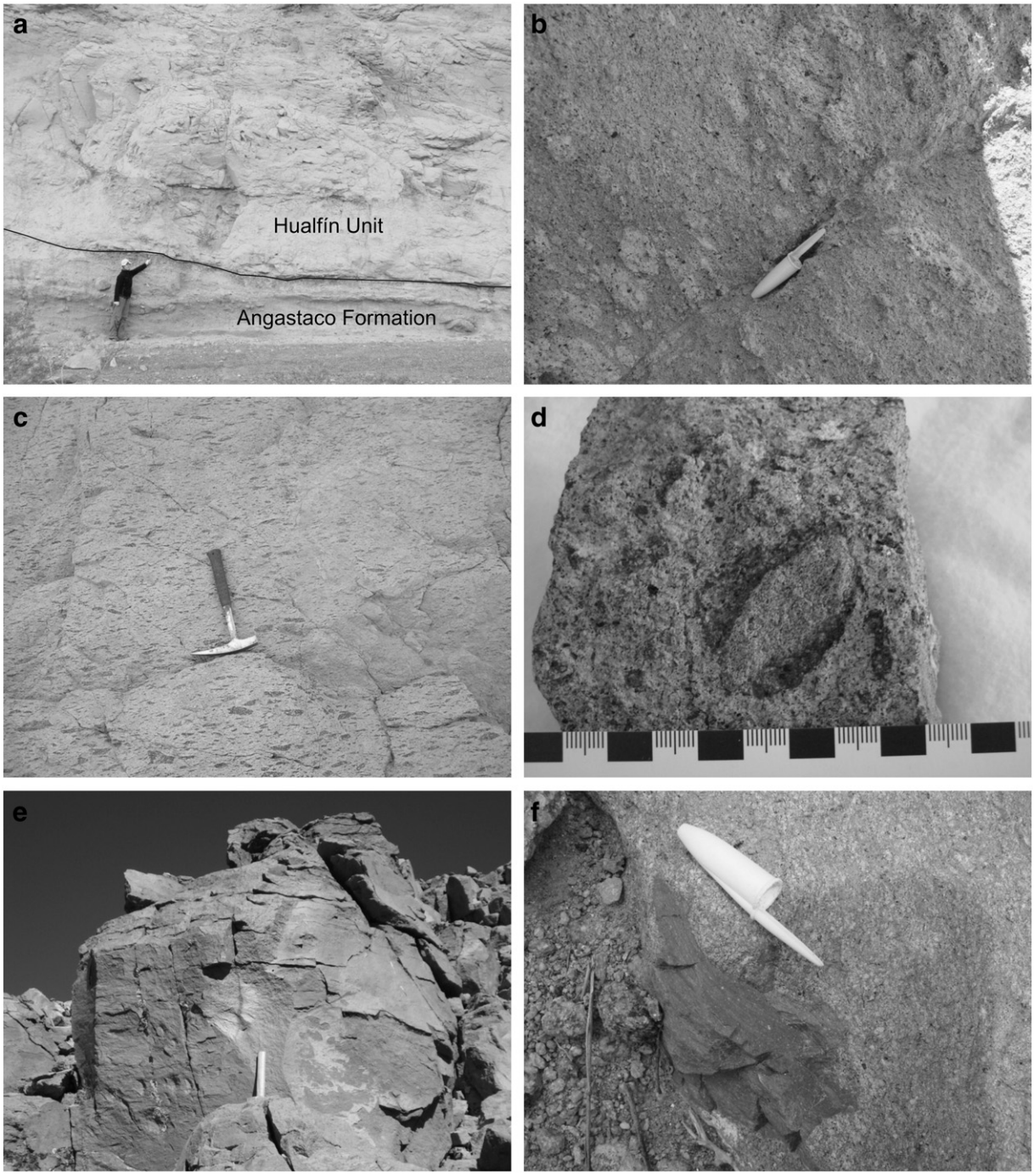

Fig. 6. Pucarilla Ignimbrite: a) Hualfín Unit: general aspect, it is an indurated massive lapilli tuff, b) some degree of flattening in pumices from the Hualfín Unit, c) eutaxitic texture in the Arremo Unit, d) Arremo Unit: detail, a grey crystal mush clast incorporated into a common fiamme; e) Jasimaná Unit, intensely welded ignimbrite, f) detail of a pink fiamme from the Jasimaná Unit.

deposits in order to determine any possible relationship. The tuffs do not belong directly to the PCTVC, but do have similar ages and are close to the ignimbrites of the PCTVC. We name these tuffs, from oldest to youngest, Tuff I, Tuff II and Tuff III.

The mineral associations of these tuffs were studied by mineral separation through densimetric and magnetometric methods. Tuff I (15.26 Ma) has an association of sphene, hornblende, clinopyroxene, zircon, rutile, apatite and abundant magnetite and ± turmaline. Tuff II (13.4 Ma) has abundant hornblende, sphene, biotite, magnetite, zircon, and ± clinopyroxene. Tuff III (middle Miocene based on its stratigraphic position) has abundant clinopyroxene and ortopyroxene, sphene, rutile, biotite, zircon, apatite and ± hornblende.

The same analysis was carried out with the PCTVC ignimbrites; results indicate the same mineral association found by petrographic analysis.

4. The Luingo caldera and the PCTVC

Detailed mapping and analysis of stratigraphic sections, facies association and characterisation, and particularly the identification of typical caldera components allow us to infer the existence of a collapse caldera (Fig. 2). As opposed to other well known collapse calderas in the Central Andes (e.g., Cerro Galán, Pastos Grandes), the Luingo caldera does not have an evident topographic expression or a satellite image outline. Therefore its identification is based upon

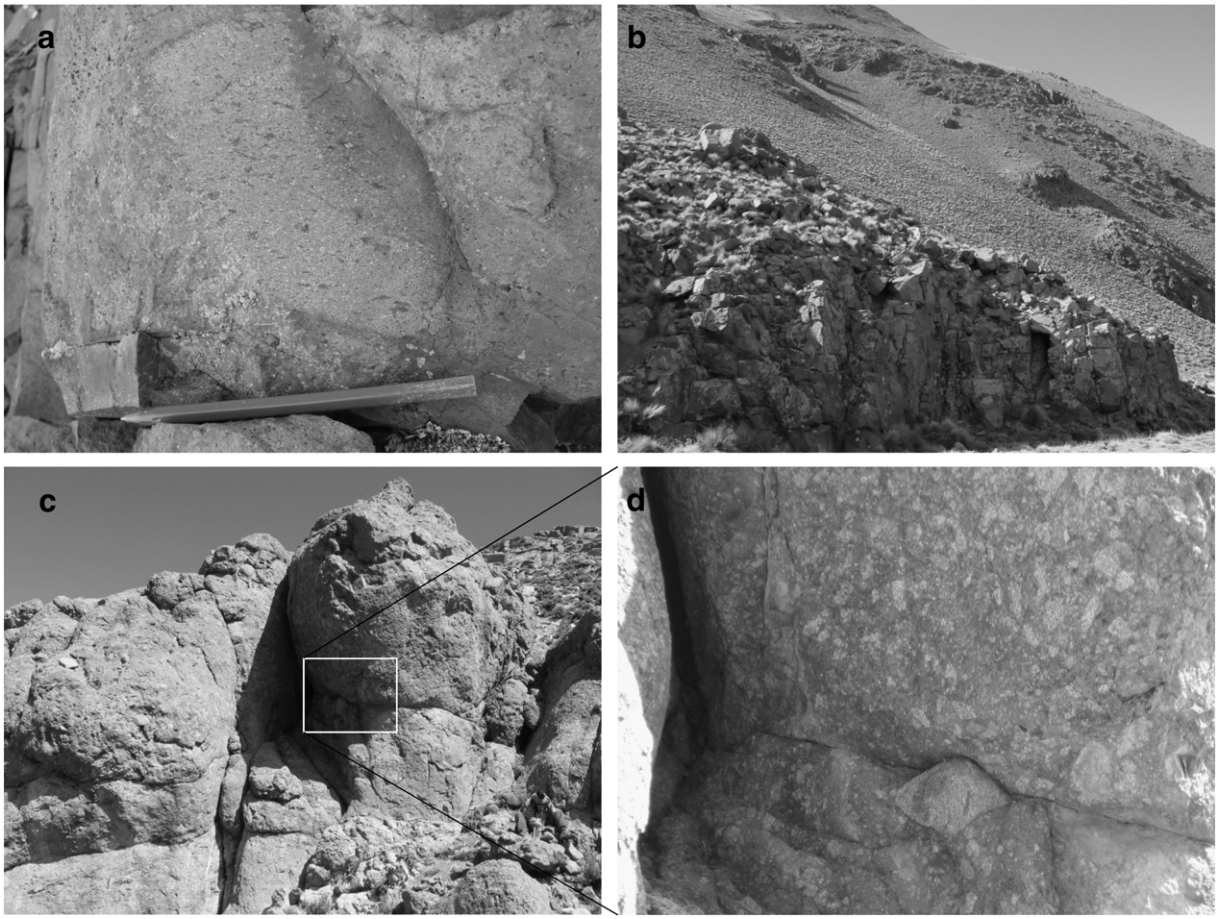

Fig. 7. a) Detail of the Luingo I Ignimbrite, showing an intense degree of welding, b) columnar jointing developed on the Luingo I Ignimbrite, c) Luingo Breccia, general appearance, d) detail of the Luingo Breccia, note sub-rounded to angular fragments within a matrix of the same composition.

detailed facies association and the survey of morphological elements in key locations.

The eastern structural side of the caldera rim (Fig. 8) is marked by the presence of a collapse breccia (Luingo Breccia) interbedded with intensely welded and hydrothermalised intracaldera tuffs (Luingo I and Luingo II ignimbrites: Figs. 9a and 10). Evidence of the western side of the rim was discerned from the presence of an arcuate fault (Fig. 8), in which intensely silicified hydrothermal breccias are hosted (Figs. 9b and 10). This fault coincides with the beginning of a topographic high made of ignimbrites and is the termination of a depression. The depression (Alto de Las Lagunas) is filled with epiclastic materials and some younger lava flows (Lavas II) suggesting that it is an intracaldera valley. Caldera axes (19 km ENE–WSW and 13 km N–S) define an elliptic caldera, elongated at a N65° trend and located at 26° 10′S–66° 40′W (coordinates of the centre of the caldera).

The distribution and characteristics of the pyroclastic deposits allow for separation into intracaldera and outflow facies. Thus, we interpret Luingo I and Luingo II Ignimbrites to be intracaldera facies, while Pucarilla and Alto de Las Lagunas Ignimbrites to be outflow facies.

Most of the features of the Alto de Las Lagunas Ignimbrite are similar to the other ignimbrites of the PCTVC, including identical pumice and lithic clasts, similar textures and structures. The Alto de Las Lagunas Ignimbrite has evident outflow characteristics (low aspect ratios, absence of generalised hydrothermal alteration and distribution around the caldera) and is located mostly towards the central-western side of the caldera. However, no intracaldera equivalent deposits have been found; these must be buried beneath the exposed intracaldera sequence.

Some uncertainty exists as to the significance of the obtained age of Alto de Las Lagunas (13.5 Ma), as no pumice separation could be carried out due to the high degree of welding of the rock samples. Field relations, facies analysis and bulk characteristics of the deposit also suggest that Alto de Las Lagunas Ignimbrite is a caldera-related ignimbrite. However, taking into account solely the ages determined for the PCTVC ignimbrites, this time period is significant enough to separate the Alto de Las Lagunas Ignimbrite from the other ignimbrites, evidence which points to similar but separate episodes. Future research should elucidate this uncertainty, but with the present data it is appropriate to consider the Alto de Las Lagunas Ignimbrite as the first pyroclastic product of the Luingo caldera.

Both the Pucarilla and the Alto Las Lagunas ignimbrites are massive lapilli tuffs, where the practical absence of vertical and lateral variations indicates that steady conditions prevailed during their sustained deposition. A low to medium aspect ratio (1.21×10^{-3}) characterises the Pucarilla Ignimbrite.

The best data for determining the eruptive history of the Luingo caldera is found on the eastern side of the caldera rim, where the intracaldera sequences are exposed (Figs. 9a and 10). The thickness and distribution of the intracaldera facies indicate a coeval caldera collapse. Thus, the sum of Luingo Breccia's characteristics, as well as its position between the Luingo I and Luingo II ignimbrites, suggest that the Luingo Breccia corresponds to a collapse breccia (c.f., Lipman, 1976) related to incremental subsidence of the caldera floor and caldera wall instability. During the eruption, the collapse magnitude increased in response to an eruption rate step-up (c.f., Druitt and Sparks, 1984). At this time big blocks of granitoids (the host rock) fell gravitationally onto the collapsed floor, covering the Luingo I

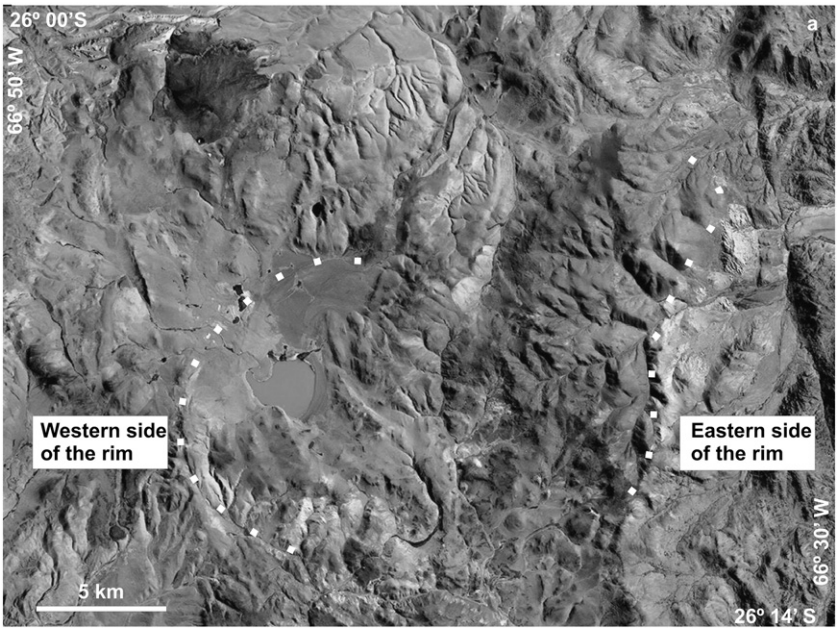

Fig. 8. Landsat 7 TM satellite image showing the Luingo caldera area; dashed line highlights the recognised caldera rim.

intracaldera Ignimbrite, and emitting the Luingo II Ignimbrite. The collapse breccia (Luingo Breccia) indicates a catastrophic topographic change, possibly associated with an increase in the conduit size (c.f., Wilson et al., 1978; Lipman, 1976; Tucker et al., 2007). The conduit enlargement was accompanied by the eruption of great volumes of magma and the deposition of a thick intracaldera ignimbrite (Luingo II) and its outflow equivalent, the Pucarilla Ignimbrite. Both the Luingo II Ignimbrite and the Luingo Breccia distributions denote the presence of an active depression at the time of this episode. The extensive and homogeneous hydrothermal alteration in the intracaldera sequence points to an active and extensive circulation of fluids, as well as a significant cooling time of the deposits at the end of the caldera cycle. Finally, lava domes, possibly partially eroded, covered the intracaldera ignimbrites.

Plume development and possible initial plinian phases in relation to the caldera-forming events were tested. The caldera event was coeval with the presence of syn-orogenic basins in the neighbouring valleys, where extensive and continuous ash-fall deposits were interbedded in the continental sequence of the upper Payogastilla Group. A comparison of mineral assemblages indicates that Tuffs I, II and III are not comparable to any of the identified PCVTC ignimbrites. Thus these ash-fall deposits are not related to the Luingo caldera episode. The thickness (ca. 1 m) and the grain size (fine ash) of these tuffs indicate that a major eruption occurred elsewhere to the west. Therefore, if the Luingo caldera episode produced plinian deposits or co-ignimbritic ashes, neither have been preserved in the sedimentary basin around the caldera.

Almost all of the pyroclastic facies of the PCTVC are highly welded ignimbrites, which reach horizontal distances of more than 35 km and have similar degrees of welding. To achieve these characteristics, a combination of factors would have played an important role in preventing heat loss, leading to high emplacement temperatures. Two likely factors were high mass eruption rate, that would make the column dense enough to produce its immediate collapse, and a small air ingestion (c.f., Smith and Bailey, 1966; Sparks and Wilson, 1976), that would have a minimum influence on the effective density of the column, thereby inhibiting the development of a high-eruptive column (c.f., Sparks and Wilson, 1976). The high-crystal content of

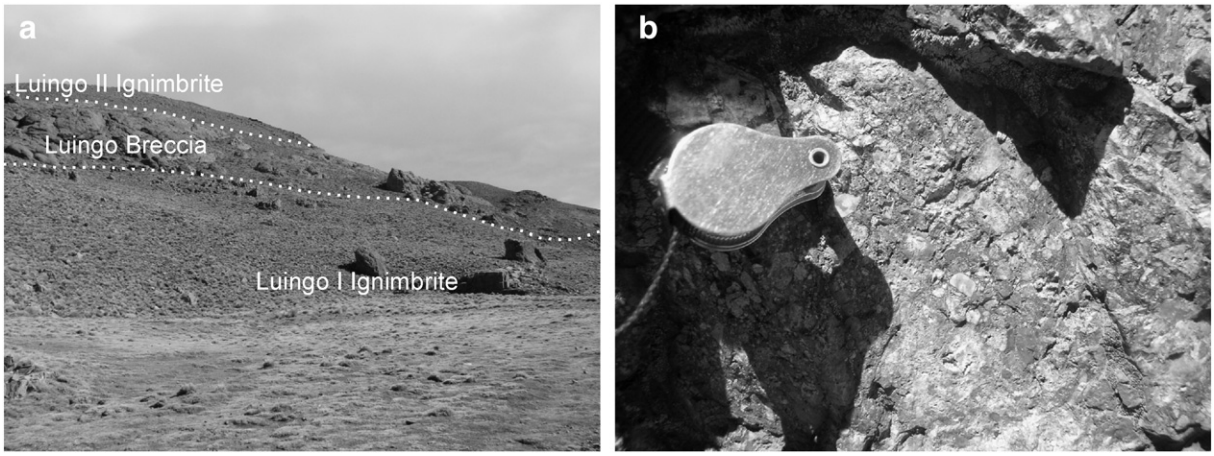

Fig. 9. a) intracaldera facies on the eastern side of the rim; collapse breccias interbedded with intensely welded tuffs, b) detail of hydrothermal breccia present on the western side of the rim.

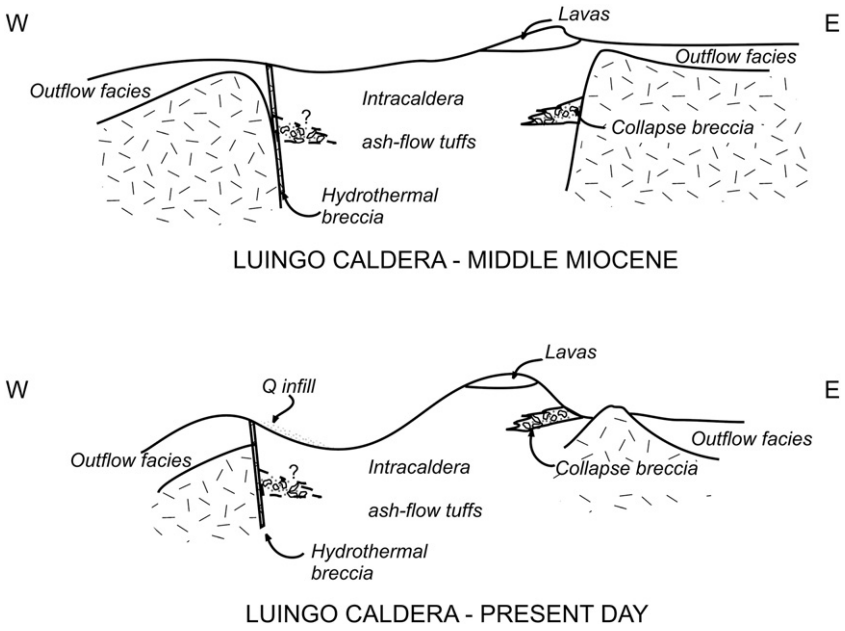

Fig. 10. Schematic cross section of the Luingo Caldera for middle Miocene and present day.

these ignimbrites (Fig. 5) elevates their bulk viscosity; thus the factors for heat preservation may have been significant. Hence, the absence of plinian deposits, the high-crystal content in pumice fragments (partially solidified magma), the persistent flattening of pumices (fiamme texture), even in distal facies (high heat retention capacity), and the immediate deposition of ignimbrites around vents points to a very low column collapsing immediately. This has been suggested for many other calderas in the CVZ (c.f., Sparks et al., 1985; de Silva, 1989; Ort, 1993; Lindsay et al., 2001a; Soler et al., 2007).

One important feature is that the recognised caldera is bounded by NW–SE regional faults (as seen in Fig. 2). Considering the high-crystal content of all the deposits related to the caldera, it is tempting to consider that these faults played a crucial role in allowing the eruption from a magma chamber with these characteristics.

The caldera has the typical characteristics of an overpressure collapse caldera according to Martí et al. (2009), including (i) an absence of plinian phases, (ii) large caldera size, (iii) important volumes of erupted magma (>100 km^3), (iv) almost all of the erupted magma accompanied caldera subsidence, (v) calc-alkaline dacitic composition, and (vi) most caldera-forming sequences correspond to syn-collapse deposits. Some features of this caldera, like the absence of fallouts beneath major ignimbrites, the crystal-rich nature of pumice, the large-volume widespread ignimbrite sheets and an evident tectonic control are indicative of fissure type eruptions (Aguirre-Díaz and Labarthe-Hernández, 2003), which in Aguirre-Díaz et al. (2008) may classify as a graben caldera.

Moreover, the Luingo caldera contains features suggesting typical trapdoor subsidence: (i) elongated configuration (c.f., Lipman, 1997), (ii) asymmetric distribution of outflow facies in plan view, concentrated in the eastern sector, and (iii) presence of a combination of well defined arcuate and linear faults and less evident structural rims, akin to those obtained by analogue models in this type of calderas (c.f., Kennedy et al., 2004).

Regarding the caldera collapse triggers, we have identified two major, possibly coeval, processes in the Luingo caldera-forming events: (i) magma recharge (Guzmán, 2009) and (ii) a syn-collapse incremental tectonic activity. Processes such as magma recharge and volatile exsolution alone are not effective or significant enough to drive eruptions in a caldera-scale crystal-rich magma chamber (Schmitt et al., 1999; Lindsay et al., 2001b; Riller et al., 2001). On the other hand, tectonic triggers in calderas that contained crystal-rich magma chambers of batholithic dimensions are well documented (e.g., Gottsmann et al., 2009). In most of the Central Andes calderas, triggers of explosive volcanism, particularly of caldera collapse, have been interpreted to be a combination of magma recharge and incremental deformation (Lindsay et al., 2001b; Riller et al., 2001; Petrinovic et al., 2005; Soler et al., 2007). Regional faults, especially in the eastern Puna border, are bi-vergent, delineating lowered basement blocks that enclose syn-tectonic basins and uplifted basement blocks that act as range-barriers (Coutand et al., 2006; Hongn et al., 2007; Strecker et al., 2009). The combination of NW–SE major faults, which have oblique components of left-lateral slip, with NE–SW faults, which have right-lateral movement, in the area and in the entire Puna–Altiplano region (e.g., Riller and Oncken, 2003; Petrinovic et al., 2005; Guzmán, 2009) reinforces the orogen-parallel stretching model proposed by Riller and Oncken (2003). Hence the rhombo-shaped geometry bounded by strike–slip faults proposed by Riller and Oncken (2003) applies favourably to the studied area and allows for favourable conditions for magma ascent.

Preliminary data suggests that a younger episode (upper Miocene) in the area is purely effusive (lavas and lava domes), and seemingly genetically unrelated to the 13–12 Ma episode. However, considering the ~7 Ma age of the ignimbrites close to the Peñas Blancas area (Castillo, 1999), a more detailed survey of the Alto Las Lagunas area could result in the recognition of an upper Miocene explosive–effusive cycle similar to the 13–12 Ma episode.

4.1. Volume of pyroclastic facies of PCTVC

Due to the low degree of preservation of the original volcanic structure and its products, volume estimations are of minimum values. Volume calculations have been based on the construction of a solid digital model of the recognised outcrops using GIS software. Limitations of this method are the uncertainties in the way elevation contours were obtained, as well as the necessary homogenisation of paleao-topography in those sectors covered by volcanic facies. Nevertheless, we were able to obtain what we consider to be adequate minimum volume estimations. The Pucarilla Ignimbrite covers a minimum area of 615 km^2; we obtained a minimum volume of 22 km^3 (20 km^3 DRE: see Appendix B). Based on the calculated

volume and area, the average thickness for this unit is 33 m, an estimation which is compatible with field observations. The calculated volume of the Alto de Las Lagunas plus the undifferentiated ignimbrites is 2 km^3.

The areal dispersion of the outflow facies could be significantly greater if the covered sectors and the areas lacking field surveys are considered. Areas to the south and west of the interpreted vent have not been surveyed, and only limited and isolated pre-existing data for these areas is available. Nevertheless, considering previous descriptions of pyroclastic rocks (Navarro García, 1984) and analysing satellite images, in these sectors we can infer the presence of considerable outcrops of pyroclastic materials related to the centre. Moreover, to the north of the caldera vast outcrops related to the Luingo caldera were most likely covered by Cerro Galán ignimbrites. In view of this, we consider that these deposits have a minimum areal dispersion of 700 km^2 and a minimum volume of 23 km^3. Outflow facies thus have a minimum volume of 50 km^3 (45 km^3 DRE) and an areal dispersion of 1 300 km^2.

Classical methods for estimating the volume of intracaldera materials (e.g., Lipman, 1997) require the knowledge of a variety of parameters (structural elements) that, based on the low degree of preservation and exposure of the volcanic structure, we are not able to calculate accurately. Lipman (1984) estimates that outflow volumes are similar to intracaldera ones. Taking this into consideration, we obtained a total (intracaldera plus outflow facies) minimum volume of 100 km^3 (90 km^3 DRE). Other authors (e.g., Lindsay et al., 2001a; Soler et al., 2007) have estimated a ratio of 2/3 of the total volume for the intracaldera facies and 1/3 for the outflow in those cases in where the caldera collapse occurred in the early stages of the eruption. We consider this approximation more appropriate for the Luingo caldera, as it has a structural control that indicates an early subsidence in the caldera evolution. We therefore estimate an intracaldera volume of 100 km^3 (90 km^3) and a total volume of 150 km^3 (135 km^3 DRE) for the deposits emitted by the Luingo caldera. It is interesting to note that this volume would give the caldera diameters of about 15 km when plotting (not shown) in Cas and Wright (1987) caldera diameter versus volume diagram.

An estimation of the minimum subsidence depth is achieved by making three assumptions. First, that the volume of the extruded material is approximately equal to the caldera volume (e.g., Amaraki, 1984), and thus the minimum magma chamber volume is 135 km^3. Second, that the depressed area of the caldera (266 km^2) is approximately equivalent to the magma chamber area in plan view (c.f., Martí et al., 1994). Third and finally, that the amount of subsidence should correspond to the height of material withdrawn from the reservoir (e.g., Martí et al., 2009). Thus we obtain a subsidence depth of 0.5 km, which is a minimum because the considered volume is the minimum value.

5. The Luingo caldera in the context of the Southern CVZ

The Luingo caldera is 20 km to the southeast of to the well known Cerro Galán caldera (Francis et al., 1980; Sparks et al., 1985). Ignimbrites from the Cerro Galán complex overlie the PCTVC ignimbrites and both share a common dispersion area. Both the Cerro Galán Complex and the PCTVC have relatively large volumes, are crystal-rich, and have mainly dacitic compositions. Magmatic activity in the Cerro Galán area has a wide spectrum of time; the well constrained effusive and explosive activity lasted from at least ~2 to 6.5 Ma (Sparks et al., 1985; Kay et al., 2008; Folkes et al., unpublished). Effusive magmatism at ~7–8 Ma (Francis et al., 1980; Schirnick and van den Bogaard, 2001; Guzmán, 2009) and isolated ages of dacitic lavas of 9.9 and 10.4 Ma (Francis et al., 1980) have been recorded. A recurrence of magmatism is evident in this area by two explosive–effusive cycles during the time periods of 2–6.5 Ma (Cerro Galán caldera: Sparks et al., 1985) and 12–14 Ma (PCTVC: Sparks et al., 1985; Marrett et al., 1994; Castillo, 1999; Folkes et al., unpublished; this work). A gap of about 5 Ma without ignimbrite-forming eruptions is apparent. Similar episodic caldera volcanism has been reported in the San Juan Volcanic Field, Colorado (e.g. Lipman, 1976; Lipman, 1984).

In the last years, several studies have been focused on the growth mechanism of sub-caldera plutons (e.g., Bachmann et al., 2002; Jellinek and DePaolo, 2003; Lipman, 2006; Bachmann and Bergantz, 2008). Caldera-forming eruptions of >100 km^3 in volume need magma to be accumulated and stored inside the chamber for long periods, such as 10^5 to 10^6 years (e.g., Jellinek and DePaolo, 2003); this is possible with an incremental growth of the pluton through recurrent magma input (e.g., Jellinek and DePaolo, 2003; Glazner et al., 2004; Lipman 2006). The lifetime of these plutons can be as large as 10 Ma (e.g. Tuolumnes Intrusive Suite: Glazner et al., 2004). If the Glazner et al. (2004) hypothesis is true, taking the volume of volcanic products from Luingo and Galán calderas into consideration, then a relationship between the Luingo caldera and Cerro Galán caldera could exist. Future work in the Cerro Galán–Luingo area could plausibly bring to light new ages of the effusive and explosive magmatism that may continue to fill this 5 Ma apparent gap in large-volume magmatism.

Our results indicate that the Luingo–Galán area is characterised by large-volume ignimbrite-forming volcanism, which is recurrent in time and in space for a period of about at least 10 Ma, with favourable conditions for the production and storage of silicic magmas and a structural framework which is favourable for caldera collapses. However no direct relation between the magma chambers that led to the caldera-forming eruptions of Galán and Luingo can be established with the available data.

6. Conclusions

This article identifies and describes the previously-unknown Luingo caldera, a collapse caldera in the southern Central Andes. Luingo is the south-easternmost (26° 10′S–66° 40′W) and oldest (12–13 Ma) recognised caldera within the Southern CVZ. It has an elongated profile at 65°N, with axes of 19×13 km, with a minimum erupted volume of 135 km^3. It is composed predominantly of dacitic, crystal-rich, welded ignimbrites and minor lavas that represent related posthumous magmatic events.

The distribution of ignimbrites and collapse deposits indicate coeval collapse and eruption. The absence of plinian or ash-fall deposits, the immediate deposition of ignimbrites around vents, and persistent fiamme textures in proximal and distal ignimbrite facies suggest a low and continuously collapsing plume, as well as a high and almost constant rate of eruption. The presence of collapse breccias on the eastern border and the concentration of outflow ignimbrites to the east of Luingo caldera suggest an asymmetric collapse, similar to trapdoor geometry. Both the Luingo and Cerro Galán calderas define a volcanic area that recorded a recurrence in magmatism for at least 10 Ma. The causes of this recurrence include favourable magma generation and storage conditions, as well as a favourable structural framework which permitted magma to ascend to the surface. However, we cannot establish a direct relationship between the magma chambers which led to the caldera-forming eruptions of Galán and Luingo with the available data.

Acknowledgments

This research was funded by PIP 5255 (CONICET) and PICT 2006-381 (ANPCyT) projects. S. Guzmán thanks R. Seggiaro and F. Hongn for helping as co advisors of the PhD thesis that led to this study. Thanks to C. Montero for redrawing the map and for the helpful discussions. Thanks to all the people that helped in the field (M. Novara, D. Riva, C. Montero, R. Chocobar, D. Vinante, A. Carabanti and F. Heit) and with the discussions (C. del Papa, M. Arnosio). Thanks to Pablo Grosse for a thorough reading of the manuscript. Thanks to J. Viramonte, H.

Wright, C. Folkes for inviting me to a field trip; to S. de Silva, C. Folkes and H. Wright for facilitating and performing a date. We thank Gerardo Aguirre-Díaz, Joan Martí and Michel Ort whose reviews greatly improved this manuscript; we also thank comments by S. de Silva on a previous version of the article.

Appendices A. Analytic methodologies for age determinations

In the present contribution we show new $^{40}Ar/^{39}Ar$ dates that were performed on biotite (Fig. 11). One belongs to lavas and two to pyroclastic rocks. The only sample from which pumices could be

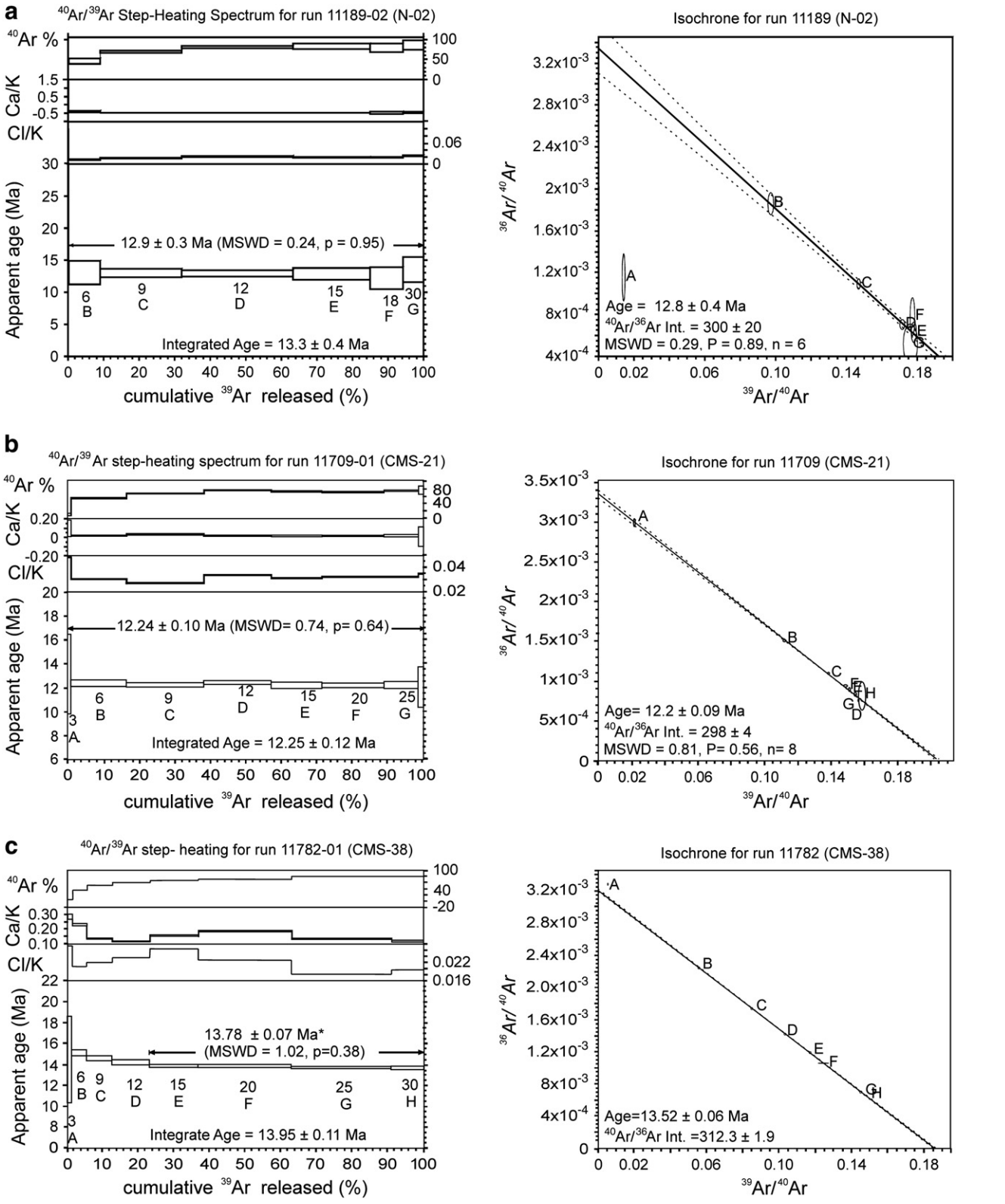

Fig. 11. $^{40}Ar–^{39}Ar$ age spectra carried out for this study. See Table 2 for a summary of $^{40}Ar–^{39}Ar$ data. a) Sample N-02, biotite of the Arremo Unit (Pucarilla Ignimbrite), b) sample CMS-21, biotite of Lavas I, and c) sample CMS-38, biotite of the Alto de Las Lagunas Ignimbrite.

separated is from the Jasimaná Unit (Folkes et al., unpublished). Samples from Lavas I, the Alto de Las Lagunas Ignimbrite and the Arremo Unit of the Pucarilla Ignimbrite were sent to the SERNAGEOMIN (Chile) laboratory where separation of minerals was performed. The applied methodology was step-wise heating. Ages from plateaus were taken as valid values for samples CMS-21 and N-02. Conditions necessary for plateau identification were: a) minimum of three consecutive steps with concordance of 2 sigma error, and b) minimum plateau length must be 50% of the cumulative ^{39}Ar released during the analysis. In the case of sample CMS-38, isochrone values were taken to be more reliable, because the sample showed a slight excess in Ar. For methodologies of the sample analysed at Oregon (P-002 from the Jasimaná Unit) see descriptions in Folkes et al. (unpublished).

Appendix B. Bulk density of the Pucarilla Ignimbrite

We estimated the density of the Pucarilla Ignimbrite using a hydrostatic weighing technique. Unaltered bulk matrix samples were selected for the procedure. The method consisted of recording the displaced volume when a sample portion of known weight had been introduced in a volumetric flask. This flask is connected to a pipette through a rubber tube. The procedure consisted of adding a known volume of distilled water to the flask, then introducing a cube of rock sample (previously weighted and covered with paraffin in order to impermeabilise it) then observing the displaced volume of water. Results indicate densities of 1.951 ± 0.04 g/cm^3 for the Hualfín Unit, 2.12 ± 0.02 g/cm^3 for the Arremo Unit and 2.348 ± 0.02 g/cm^3 for the Jasimaná Unit. The density increase is clearly proportional to the increment in the degree of welding.

Considering that the average density of dacites is around 2.6 g/cm^3 with these results we obtained conversion factors of 0.75, 0.81 and 0.9 for the Hualfín, Arremo and Jasimaná units respectively by calculating DRE volumes. However, as the Jasimaná Unit is by far the most important volumetrically, whenever we estimated the DRE volumes we used the Jasimaná data for the calculation.

References

Aceñolaza, F.G., Toselli, A.J., González, O., 1976. Geología de la región comprendida entre el salar del Hombre Muerto y Antofagasta de la Sierra, provincia de Catamarca. Rev. Asoc. Geol. Argent. 31 (2), 127–136.

Aguirre-Díaz, G.J., Labarthe-Hernández, G., 2003. Fissure ignimbrites: fissure-source origin for voluminous ignimbrites of the Sierra Madre Occidental and its relationship with Basin and Range faulting. Geology 31, 773–776.

Aguirre-Díaz, G.J., Labarthe-Hernández, G., Tristán-González, M., Nieto-Obregón, J., Gutiérrez-Palomares, I., 2008. The ignimbrite flare-up and graben-calderas of the Sierra Madre Occidental, Mexico. In: Gottsmann, J., Martí, J. (Eds.), Caldera Volcanism: Analysis, Modelling and Response, Developments in Volcanology 10. Elsevier, Amsterdam, pp. 143–180.

Amaraki, S., 1984. Formation of the Aira caldera, southern Kyushu, 22,000 years ago. J. Geophys. Res. 89, 8485–8501.

Bachmann, O., Bergantz, G., 2008. The magma reservoirs that fed supereruptions. Elements 4, 17–21.

Bachmann, O., Dungan, M.A., Lipman, P.W., 2002. The Fish Canyon magma body, San Juan volcanic field, Colorado: rejuvenation and eruption of an upper crustal batholithic magma chamber. J. Petrol. 43, 1469–1503.

Blasco, G., Zappettini, E., 1996. Hoja Geológica 2566-I (1:250.000) San Antonio de los Cobres, provincias de Salta y Jujuy, 217. Dirección Nacional del Servicio Geológico, boletín, Buenos Aires, p. 126.

Camacho de Alcalde, M., 1977. Estudio geológico del borde oriental de los valles Calchaquíes, entre Amblayo y San Carlos (provincia de Salta). Revista del Instituto de Geología y Minería de Jujuy, 2. Universidad Nacional de Jujuy, pp. 71–103.

Carrera, N., Muñoz, J.A., 2008. Thrusting evolution in the southern Cordillera Oriental (northern Argentine Andes): constraints from growth strata. Tectonophysics 459 (1–4), 107–122.

Cas, R.A.F., Wright, J.W., 1987. Volcanic Successions: Modern and Ancient. Unwin Hyman, London. 528 pp.

Castillo, A.L., 1999. El Complejo Granítico Peñas Blancas, Jasimaná, Salta: petrografía y mineralizaciones. 14° Congreso Geológico Argentino, Actas 2, La Plata, pp. 155–158.

Castillo, A.L., Aguilera, N., 1988. Geología Económica de Jasimaná, Provincia de Salta. 3° Congreso de Geología Económica, Olavarría, pp. 347–367.

Coutand, I., Carrapa, B., Deeken, A., Schmitt, A., Sobel, E., Strecker, M., 2006. Propagation of orographic barriers along an active range front: insights from sandstone petrography and detrital apatite fission-track thermocrhonology in the intramontane Angastaco basin, NW Argentina. Basin Res. 18, 1–26.

de Silva, S.L., 1989. Altiplano–Puna Volcanic Complex of the Central Andes. Geology 17, 1102–1106.

de Silva, S.L., Francis, P.W., 1991. Volcanoes of the Central Andes. Springer-Verlag, Berlin.

Díaz, J., Malizzia, D., 1984. Estudio geológico y sedimentológico del Terciario Superior del Valle Calchaquí (Departamento de San Carlos, Prov. de Salta). Boletín Sedimentológico 2 (1), 8–28.

Druitt, T.H., Sparks, R.S.J., 1984. On the formation of calderas during ignimbrite eruptions. Nature 310, 679–681.

Folkes, C., Wright, H.M., Cas, R.A.F., de Silva, S.L., Lesti, C., Viramonte, J.G., submitted for publication. A re-appraisal of the stratigraphy and deposit volumes in the Cerro Galán volcanic system, NW Argentina. Bull. Volcanol.

Francis, P.W., Thorpe, R.S., Moorbath, S., Kretzschmar, G.A., Hammill, M., 1980. Strontium isotope evidence for crustal contamination of calc-alkaline volcanic rocks from Cerro Galan, northwest Argentina. Earth Planet. Sci. Lett. 48, 257–267.

Glazner, A.F., Bartley, J.M., Coleman, D.S., Gray, W., Taylor, R.Z., 2004. Are plutons assembled over millions of years by amalgamation from small magma chambers? GSA Today 14 (4–5), 4–11.

González, O.E., 1992. Geología de a Puna Austral entre los 25° 15′ a 26° 30′ de latitud Sur y los 66° 25′a 68° 00′ de Longitud Oeste, Provincias de Catamarca y Salta, Argentina. Acta Geol. Lilloana 17 (2), 63–88.

González, O.E., Viruel, M.E., Fernández, D.S., 1999. El complejo piroclástico Cerro Tipillas en el borde oriental de la Puna Austral, Argentina, 2. 14° Congreso Geológico Argentino, La Plata, pp. 236–239.

Gottsmann, J., Lavallée, Y., Martí, J., Aguirre-Díaz, G., 2009. Magma–tectonic interaction and the eruption of silicic batholiths. Earth Planet. Sci. Lett. 284, 426–434.

Grier, M., Dallmeyer, R.D., 1990. Age of the Payogastilla Group: implications for foreland basin development, NW Argentina. J. South. Am. Earth. Sci. 3, 269–278.

Guzmán, S., 2009. Petrología y relaciones tectono-magmáticas del Complejo Volcánico Pucarilla-Cerro Tipillas, Provincia de Salta. Ph. D. Thesis, Universidad Nacional de Salta, Argentina

Hongn, F.D., Seggiaro, R., 2001. Hoja Geológica 2566—III. Cachi. Boletín No. 248. Programa Nacional de Cartas Geológicas 1:250.000. SEGEMAR, Argentina.

Hongn, F., del Papa, C., Powell, J., Petrinovic, I., Mon, R., Deraco, V., 2007. Middle Eocene deformation and sedimentation in the Puna–Eastern Cordillera transition (23°–26° S): control by preexisting heterogeneities on the pattern of initial Andean shortening. Geology 35 (3), 271–274.

Hongn, F., Mon, R., Petrinovic, I., del Papa, C., Powell, J., 2008. Inversion tectónica en el noroeste argentino: Influencia de las heterogeneidades del basamento. XVII Congreso Geológico Argentino, Actas III, Jujuy, pp. 25–27.

Jellinek, A.M., DePaolo, D.J., 2003. A model for the origin of large silicic magma chambers: precursors of caldera-forming eruptions. Bull. Volcanol. 65, 363–381.

Kay, S.M., Coira, B., Woerner, G., Singer, B.S., 2008. Cerro Galán Ignimbrite: trace element, isotopic and 40Ar/39Ar age constraints on the evolution of the central Andean Lithosphere. American Geophysical Union, Fall Meeting 2008. abstract #V22A-06. http://adsabs.harvard.edu/abs/2008AGUFM.V22A.06 K.

Kennedy, B., Stix, J., Vallance, J.W., Lavallée, Y., Longpre, M.A., 2004. Controls on caldera structure: results from analogue sandbox modeling. Geol. Soc. Am. Bull. 116, 515–524.

Lindsay, J.M., de Silva, S., Trumbull, R., Emmermann, R., Wemmer, K., 2001a. La Pacana caldera, N. Chile: a re-evaluation of the stratigraphy and volcanology of one of the world's largest resurgent caldera. J. Volcanol. Geotherm. Res. 106, 145–173.

Lindsay, J.M., Schmitt, A.K., Trumbull, R.B., de Silva, S.L., Siebel, W., Emmermann, R., 2001b. Magmatic evolution of the La Pacana caldera system, Central Andes, Chile: compositional variation of two cogenetic, large-volume felsic ignimbrites. J. Petrol. 42 (3), 459–486.

Lipman, P., 1976. Caldera-Collapse breccias in the western San Juan Mountains, Colorado. Geol. Soc. Am. Bull. 87, 1397–1410.

Lipman, P.W., 1984. The roots of ash flow calderas in western North America: windows into the tops of granitic batholiths. J. Geophys. Res. 89, 8801–8841.

Lipman, P.W., 1997. Subsidence of ash-flow calderas: relation to caldera size and magma-chamber geometry. Bull. Volcanol. 59, 198–218.

Lipman, P.W., 2006. Incremental assembly and prolonged consolidation of Cordilleran magma chambers: evidence from the Southern Rocky Mountain volcanic field. Geosphere 3 (1), 42–70.

Marrett, R., Allmendinger, R., Alonso, R., Drake, R., 1994. Late Cenozoic tectonic evolution of the Puna Plateau and adjacent foreland, northwestern Argentine Andes. J. S. Am. Earth Sci. 7 (2), 179–207.

Martí, J., Ablay, G.J., Redshaw, L.T., Sparks, R.S.J., 1994. Experimental studies of collapse calderas. J. Geol. Soc. Lond. 151, 919–929.

Martí, J., Geyer, A., Folch, A., 2009. A genetic classification of collapse calderas based on field studies, and analogue and theoretical modelling. In: Thordarson, T., Self, S., Larsen, G., Rowland, S.K., Hoskuldsson, A. (Eds.), Studies in Volcanology: The Legacy of George Walker. Special Publications of IAVCEI, 2. Geological Society, London, pp. 249–266.

Mc Arthur, A.N., Cas, R.A.F., Orton, G.J., 1998. Distribution and significance of crystalline, perlitic and vesicular textures in the Ordovician Garth Tuff (Wales). Bull. Volcanol. 60, 260–285.

Mortimer, E., Carrapa, B., Coutand, I., Schoenbohm, L., Sobel, E., Sosa Gómez, J., Strecker, M., 2007. Fragmentation of a foreland basin in response to out-of-sequence basement uplifts and structural reactivation: El Cajón-Campo del Arenal basin, NW Argentina. Geol. Soc. Am. Bull. 119 (5/6), 637–653.

Navarro García, L., 1984. Estratigrafía de la región comprendida entre los paralelos de 26° 00′ a 26°15′ de latitud sur y los meridianos de 66° 30′ a 67° 00′ de longitud

oeste, provincia de Catamarca, 1. Actas 9° Congreso Geológico Argentino, Bariloche, pp. 353–383.
Ort, M., 1993. Eruptive processes and caldera formation in a nested downsag collapse caldera: Cerro Panizos, central Andes Mountains. J. Volcanol. Geotherm. Res. 56: 295-221-252.
Pereyra, R., Becchio, R., Viramonte, J.G., Pimentel, M., 2008. Minerales pesados en depósitos piroclásticos de caída distales, su uso en la correlación crono-estratigráfica entre la Formación Angastaco (Grupo Payogastilla) y Formación Anta (Grupo Orán). Actas del 17° Congreso Geológico Argentino. Tomo 1, Jujuy, pp. 227–228.
Petrinovic, I.A., Mitjavila, J., Viramonte, J.G., Martí, J., Becchio, R., Arnosio, M., Colombo, F., 1999. Geoquímica y Geocronología de secuencias volcánicas Neógenas de trasarco, en el extremo oriental de la Cadena Volcánica Transversal del Quevar, noroeste de Argentina. Acta Geológica Hispánica: Geología de los Andes Centrales Meridionales: El Noroeste Argentino, 34, pp. 255–273. 2–3.
Petrinovic, I.A., Riller, U., Brod, J.A., 2005. The Negra Muerta volcanic complex, southern Central Andes: geochemical characteristics and magmatic evolution of an episodically volcanic centre. J. Volcanol. Geotherm. Res. 140, 295–320.
Petrinovic, I.A., Martí, J., Aguirre-Díaz, G.J., Guzmán, S.R., Geyer, A., Salado Paz, N., 2010. The Cerro Aguas Calientes caldera, NWArgentina: an example of a tectonically controlled polygenetic collapse caldera, and its regional significance. J. Volcanol. Geotherm. Res. 194, 15–26.
Riller, U., Oncken, O., 2003. Growth of the central Andean plateau by tectonic segmentation is controlled by the gradient in crustal shortening. J. Geol. 111, 367–384.
Riller, U., Petrinovic, I., Ramelow, J., Strecker, M., Oncken, O., 2001. Late Cenozoic tectonism, caldera and plateau formation in the Central Andes. Earth Planet. Sci. Lett. 188, 299–311.
Ross, C.S., Smith, R.L., 1961. Ash-flow tuffs, their origin, geologic relations and identification. U.S. Geol. Surv. Prof. Pap. 366.
Schirnick, C., van den Bogaard, P., 2001. The Cerro Galán Caldera (NW Argentina), a Longer Valley of the Andes? A 6 m.y. record of large-volume rhyodacite eruptions from a mature silicic magma system. Abstracts, Penrose Conference on Longevity and Dynamics of Rhyolitic Magma Systems, Mammoth, California.
Schmitt, A., Lindsay, J. M., Emmermann, R., 1999. Pre-eruptive Magma Storage Conditions and Evidence for Externally Controlled Eruption of Large-volume Central Andean Ignimbrites. Dissertation, AGU Fall Meeting
Schnurr, W., Trumbull, R., Clavero, J., Hahne, K., Siebel, W., Gardeweg, M., 2007. Twenty-five million years of silicic volcanism in the southern central volcanic zone of the Andes: geochemistry and magma genesis of ignimbrites from 25 to 27° S, 67 to 72° W. J. Volcanol. Geotherm. Res. 166, 17–46.
Seggiaro, R., Brandán, E.M., Guzmán, S., 2006. Inversión Tectónica del Cerro Colorado, Departamento San Carlos, Provincia de Salta. Resúmenes expandidos 13° Reunión de Tectónica, San Luis.
Siebel, W., Schnurr, W., Hahne, K., Kraemer, B., Trumbull, R., van den Bogaard, P., Emmermann, R., 2001. Geochemistry and isotope systematics of small to medium volume Neogene Quaternary ignimbrites in the southern central Andes: evidence for derivation from andesitic magma sources. Chem, Geol 171, 213–217.
Smith, R.L., Bailey, R.A., 1966. The Bandelier Tuff: a study of ash-flow eruption cycles from zoned magma chamber. Bull. Volcanol. 29, 83–103.
Soler, M.M., Caffe, P.J., Coira, B.L., Onoe, A.T., Kay, S.M., 2007. Geology of the Vilama caldera: a new interpretation of a large-scale explosive event in the Central Andean plateau during the Upper Miocene. J. Volcanol. Geotherm. Res. 164 (1–2), 23–53.
Sparks, R.S.J., Wilson, L., 1976. A model for the formation of ignimbrite by gravitational column collapse. J. Geol. Soc. Lond. 132, 441–451.
Sparks, R., Francis, P., Hamer, R., Pankhurst, R., O´Callaghan, L., Thorpe, R.S., Page, R., 1985. Ignimbrites of the Cerro Galán caldera, NW Argentina. J. Volcanol. Geotherm. Res. 24, 205–224.
Strecker, M.R., Alonso, R., Bookhagen, B., Carrapa, B., Coutand, I., Hain, M.P., Hilley, G.E., Mortimer, E., Schoenbohm, L., Sobel, E.R., 2009. Does the topographic distribution of the central Andean Puna Plateau result from climatic or geodynamic processes? Geology 37, 643–646.
Thorpe, R.S., Francis, P.W., O´Callaghan, L.O., 1984. Relative roles of source composition, fractional crystallization and crustal contamination in the petrogenesis of Andean volcanic rocks. Philos. Trans. R. Soc. (Lond.) 310, 675–692.
Tucker, D., Hildreth, W., Ullrich, T., Friedman, R., 2007. Geology and complex collapse mechanisms of the 3.72 Ma Hannegan caldera, North Cascades, Washington, USA. Geol. Soc. Am. Bull. 119 (3/4), 329–342.
Turner, J.C., 1962. Estratigrafía de la región al naciente de la Laguna Blanca (Catamarca). Rev. Asoc. Geol. Argent. 18 (1–2), 11–45.
Viramonte, J.M., Becchio, R., Viramonte, J.G., Pimentel, M., Martino, R., 2007. Ordovician igneous and metamorphic units in southeastern Puna: New U–Pb and Sm–Nd data and implications for the evolution of Northwestern Argentina. J. South. Am. Earth Sci. 24, 167–183.
Wilson, L., Sparks, R.S.J., Huang, T.C., Watkins, N.D., 1978. The control of eruption column heights by eruption energetics and dynamics. J. Geophys. Res. 83, 1829–1836.